Proton Form Factors and Two-Photon-Exchange

H. Czyz
Institute of Physics, University of Silesia, 40007 Katowice, Poland

L. Xia1, D. Liu, Q. Q. Song, X. R. Zhou, P. L. Li, G. S. Huang, Z. G. Zhao, H. P. Peng, W. B. Yan
University of Science and Technology of China
State Key Laborator of Particle Detection and Electronics

J. F. Hu, H. J. Yang
Shanghai Jiao Tong University
Key Laboratory for Particle Physics, Astrophysics and Cosmology, Ministry of Education
Shanghai Key Laboratory for Particle Physics and Cosmology; Institute of Nuclear and Particle Physics

Y.D. Wang, C. Morales, C. Rosner and, A. Dbeyssi, S. Ahmed, P. Larin, Frank Maas
Helmholtz-Institute Mainz
Johannes Gutenberg University

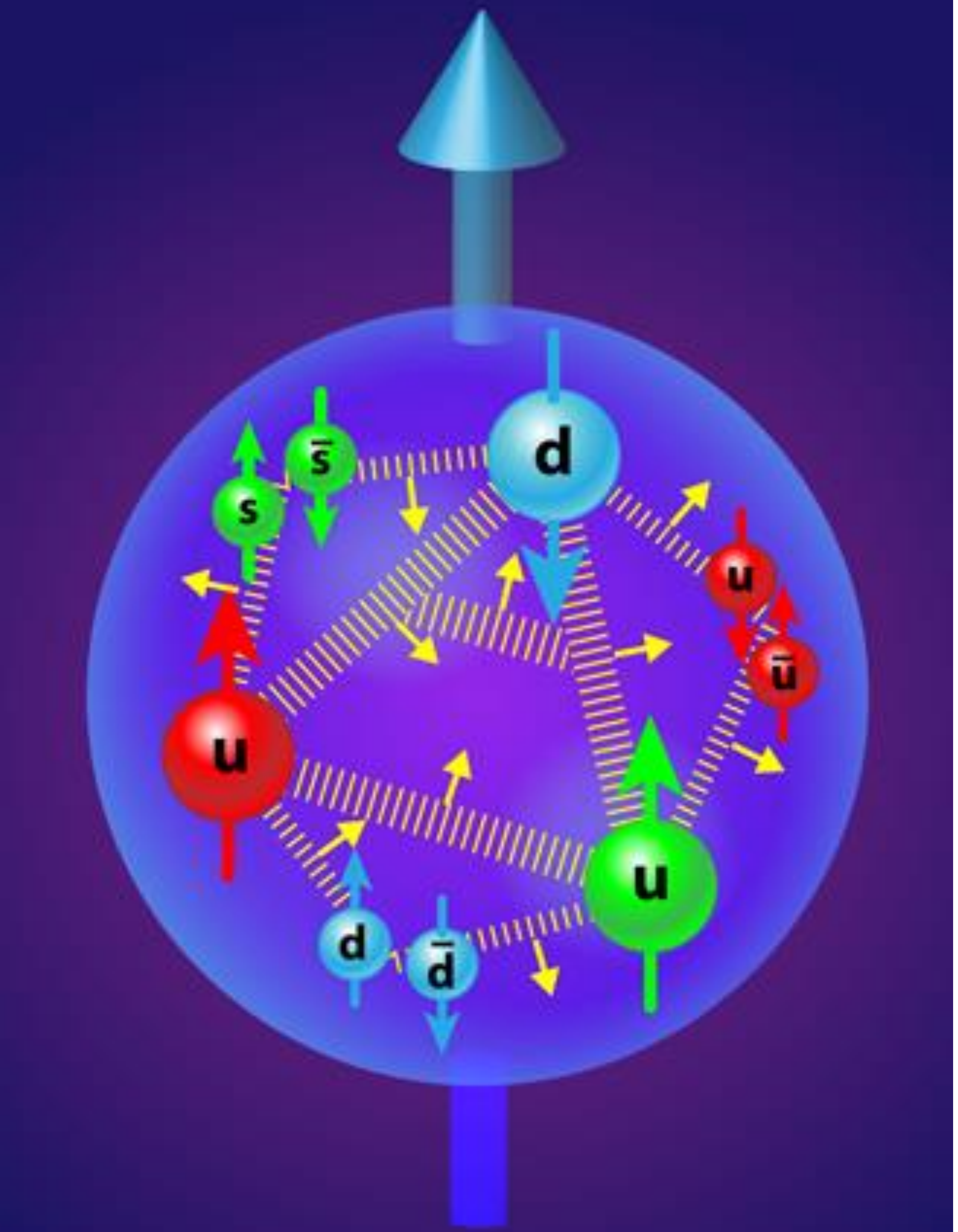

Proton Form Factors

- Non-point like particle and its structure and dynamics can be described by:
  - Electromagnetic form factors
  - Parton Distribution Functions
  - Generalized Parton Distributions
  - ……
- By performing a global analysis on the data from scattering and annihilation experiments, one can determine these functions and well understand its structure.

Electromagnetic Form Factors

- characterize the internal structure and dynamics of proton:
  - At low q^2: they are related to the charge and magnetization distributions inside and hence probe the size of the proton.
  - In the limit of q^2 goes to 0: determine the charge radius.
  - At high q^2: improve our understanding of QCD and testing its scaling.
- Two Form Factors (2S+1).

Electromagnetic Form Factors

matrix element

$$\frac{e^2}{q^2}\ \bar{u}(k_2)\gamma_\mu u(k_1)\ \ \bar{u}(p_2)[\boxed{F_1}(q^2)\gamma_m u + i\kappa\frac{\sigma_{\mu\nu}q^\nu}{2m_p}\boxed{F_2}(q^2)]u(p_1)$$

Dirac

$G_E = F_1 + F_2$

$G_M = F_1 + \tau F_2$

Pauli

hadronic vector current: two form factors (2 s + 1)

internal structure of hadron ground state

Dirac	Pauli
$F_1^p(q^2=0) = 1$	$F_2^p(q^2=0) = 1$
$F_1^n(q^2=0) = 0$	$F_2^n(q^2=0) = 1$

Combination of Pauli and Dirac leads to the so called Sachs FFs:

$G_E=F_1(q^2)+(q^2/4M^2)F_2(q^2)$ $\qquad$ $G_M=F_1(q^2)+F_2(q^2)$

all hadronic structure and strong interaction in form factors, but subject to electromagnetic (QED) radiative corrections

Electromagnetic Form Factors

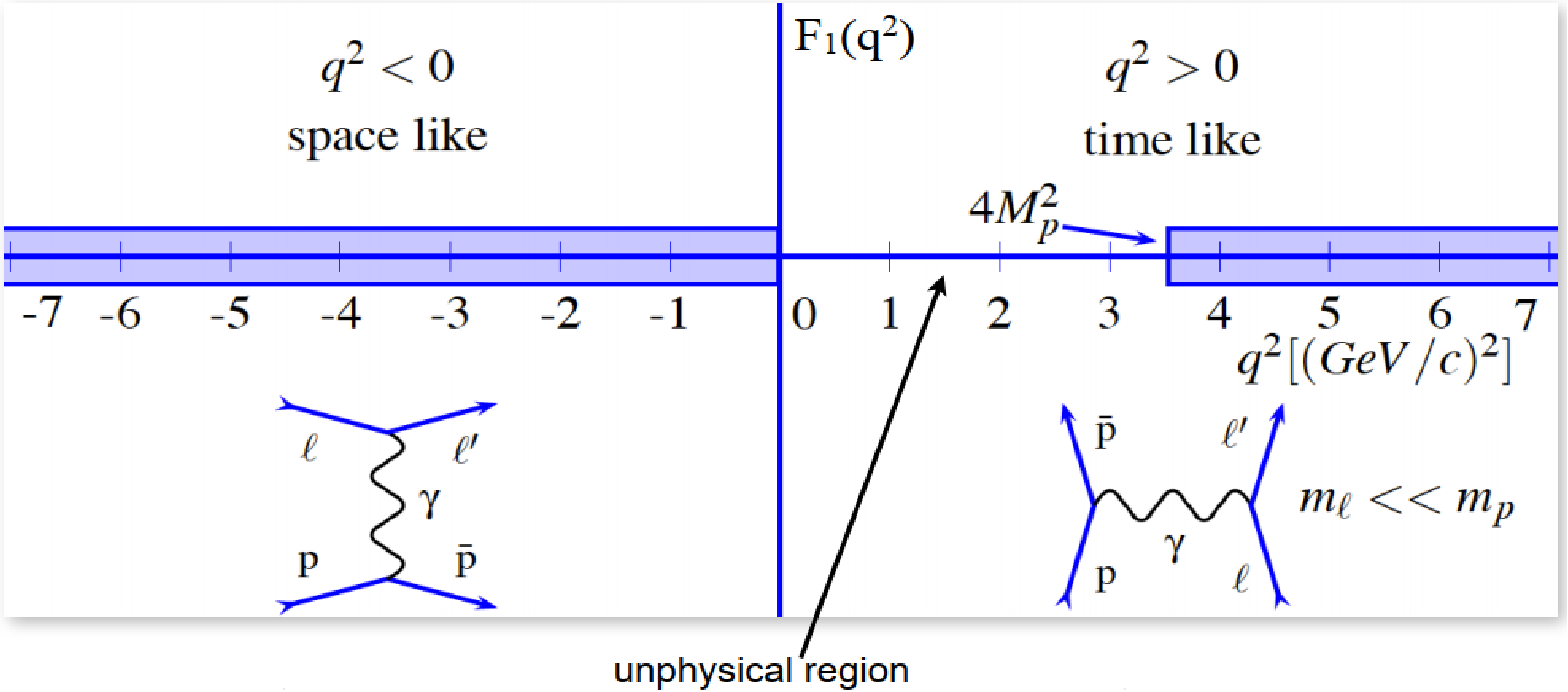

Form Factors real
cross section (Rosenbluth)
no single spin observables
double spin observables

← dispersion relations →

Form Factor complex
cross section (angular Distr.)
single spin observables (Py)
double spin observables

Electromagnetic Form Factors

Experimental observables

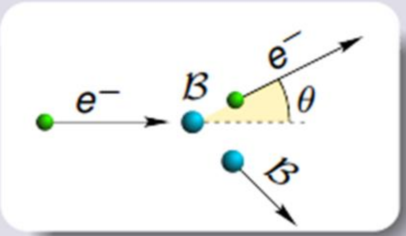

Elastic scattering

$$\frac{d\sigma}{d\Omega} = \frac{\alpha^2 E_e' \cos^2\frac{\theta}{2}}{4E_e^3 \sin^4\frac{\theta}{2}} \left[G_E^2 - \tau\left(1 + 2(1-\tau)\tan^2\frac{\theta}{2}\right) G_M^2 \right] \frac{1}{1-\tau}$$

$$\tau = \frac{q^2}{4M_{\mathcal{B}}^2}$$

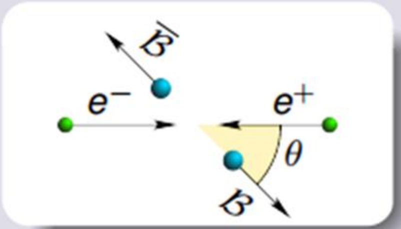

Annihilation

Coulomb correction

$$\frac{d\sigma}{d\Omega} = \frac{\alpha^2 \beta C}{4q^2} \left[(1+\cos^2\theta)|G_M|^2 + \frac{1}{\tau}\sin^2\theta |G_E|^2 \right]$$

$$\beta = \sqrt{1 - \frac{1}{\tau}}$$

Hot topics in EM Form Factor research: G_E/G_M, charge radius, unphysical region, threshold behavior, radiative corrections, two-photon exchange, large Q^2, interference

Electromagnetic Form Factors in time-like region

Direct scan

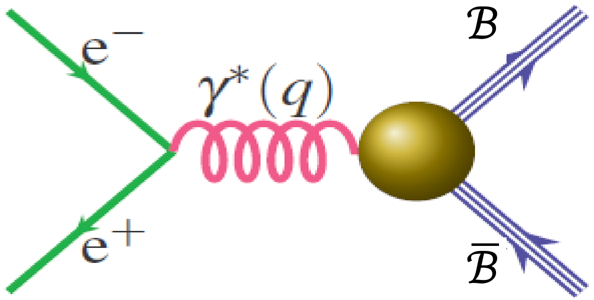

Initial State Radiation

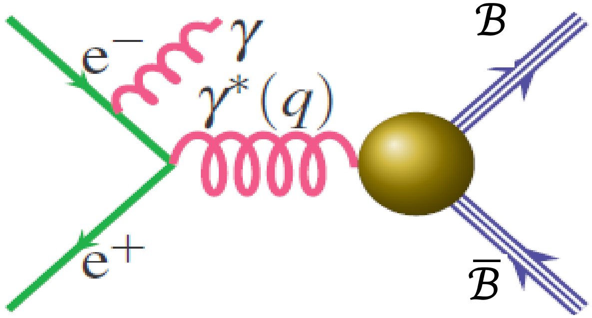

- E_{beam} discrete $\rightarrow$ **q^2 fixed**
- 'High' cross section (**~pb**)
- High geometrical acceptance

- E_{beam} fixed $\rightarrow$ **q^2 continuous**, depends on the energy carried by the ISR photon
- 'Small' cross section (**~10^{-3}pb**)
- Small geometrical acceptance: **ISR photon** emitted at **very large or very small polar angles**

Electromagnetic Form Factors in time-like region

Direct scan

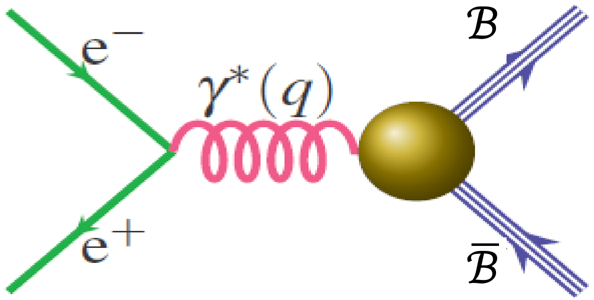

- E_{beam} discrete $\rightarrow q^2$ fixed

  → **q very precise: (~0.1 MeV)**
  ideal for $G_{E,M}$, thresholds studies

- 'High' cross section (~pb)

  → **Low luminosities needed for high statistics**

- High geometrical acceptance

  → **High detection effiicency**

Initial State Radiation

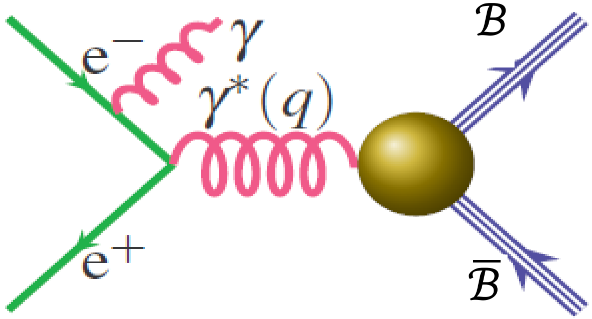

- E_{beam} fixed $\rightarrow q^2$ continuous, depends on the energy carried by the ISR photon

  → **Wide q-range available: $m_{threshold} < q < \sqrt{s}$**

- 'Small' cross section (~10^{-3}pb)

  → **High luminosities needed**

- Small geometrical acceptance: ISR photon emitted at very large or very small polar angles

  → **Threshold accessible!!**

BEPCII and BESIII

- A unique e^+e^- machine in the **τ-charm** energy region.
- **High luminosity**: 10^{33} $cm^{-2}s^{-1}$ @ 3.77 GeV
- **Excellent and stable** detector performance: 2009-now
- Studies at the near-threshold energy: $\sqrt{s}$ = **2~4.6** GeV
- **Clean environment** and well controlled initial states

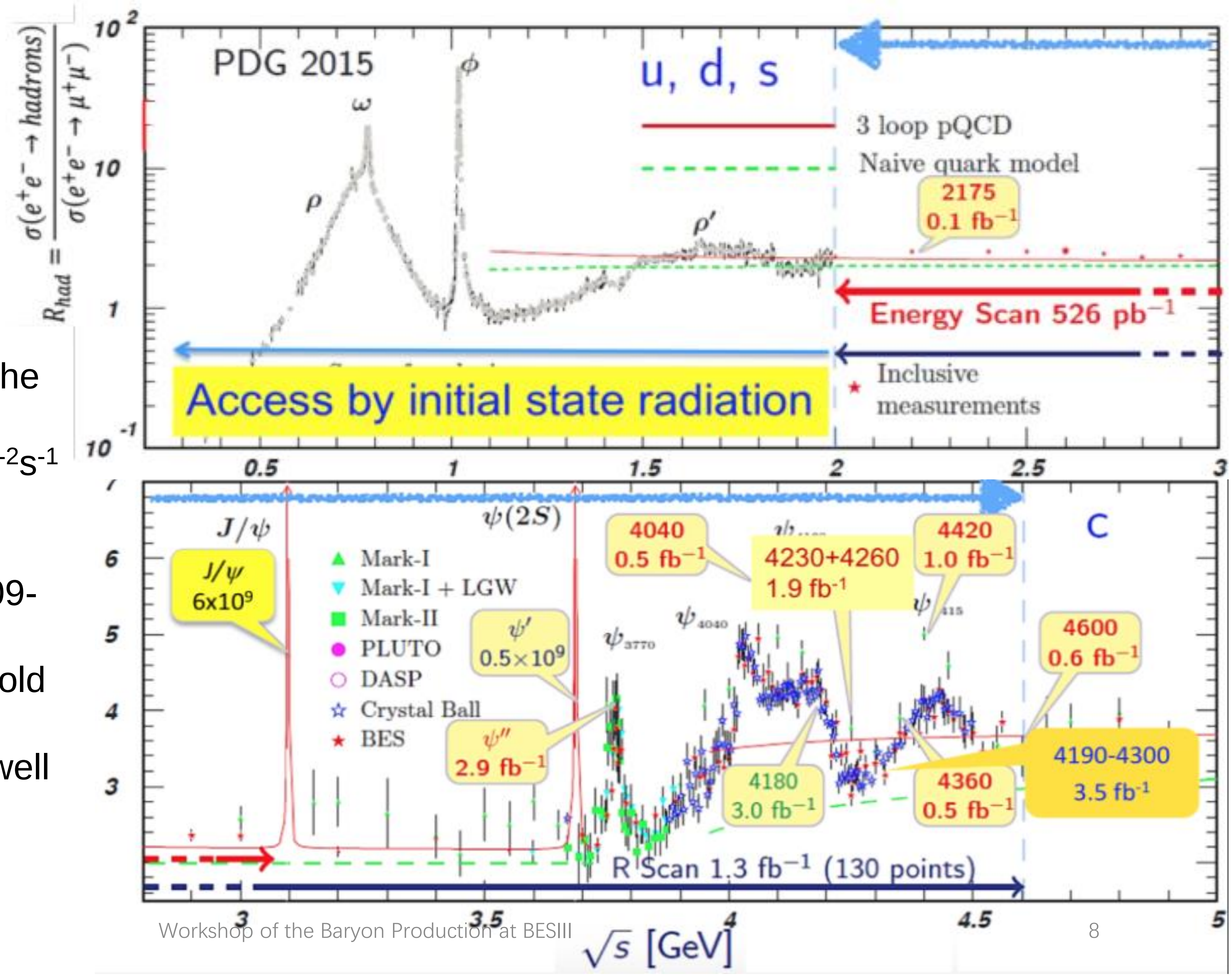

Status of p$\bar{p}$ cross section at BESIII

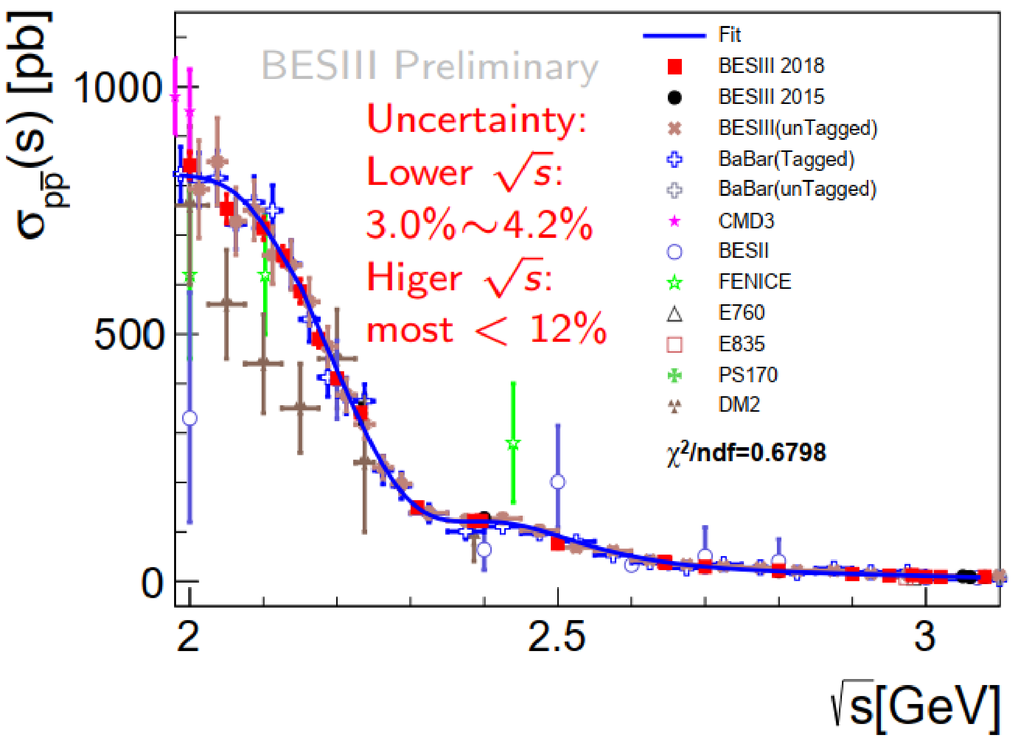

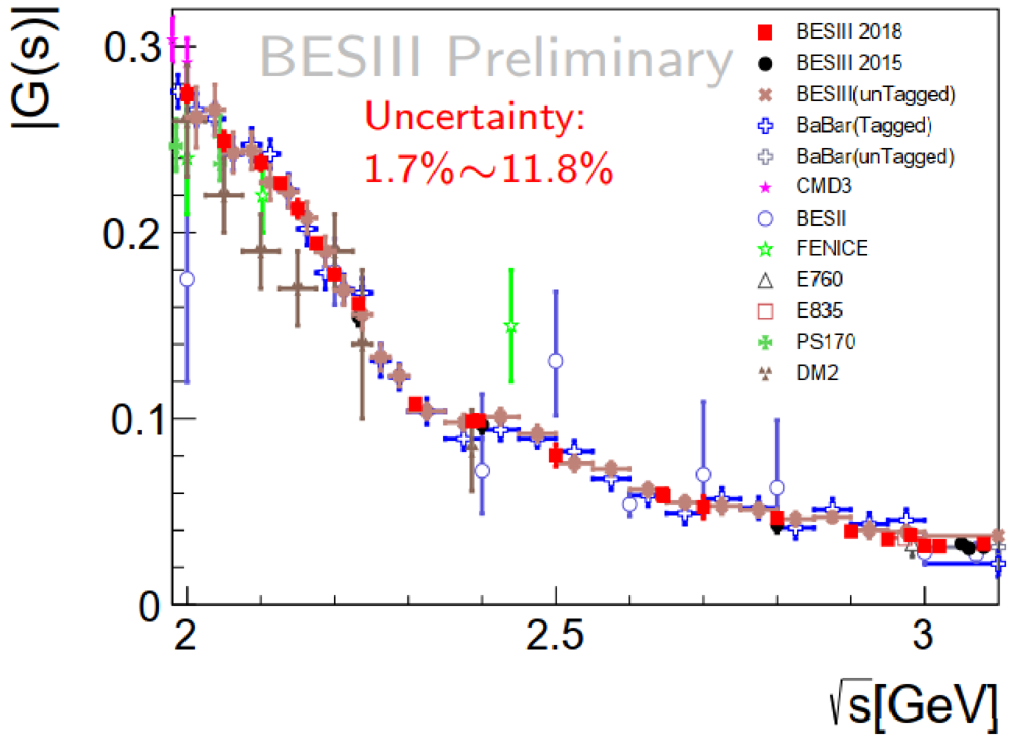

BESIII results on the cross section and effective form factor

- Direct scan method:
  - 2012 data, 156.7 pb-1, PRD 91,112004 (2015);
  - 2015 data, 668.5 pb-1, arXiv:1905.09001 (most recent and precise results.)
- Initial state radiation method:
  - Untagged analysis: data at [3.773-4.60] GeV, 7.4 pb-1, Phys. Rev. D 99, 092002;
  - Tagged analysis: data at [3.773-4.60] GeV, 7.4 pb-1, under review.

Status of $p\bar{p}$ cross section at BESIII

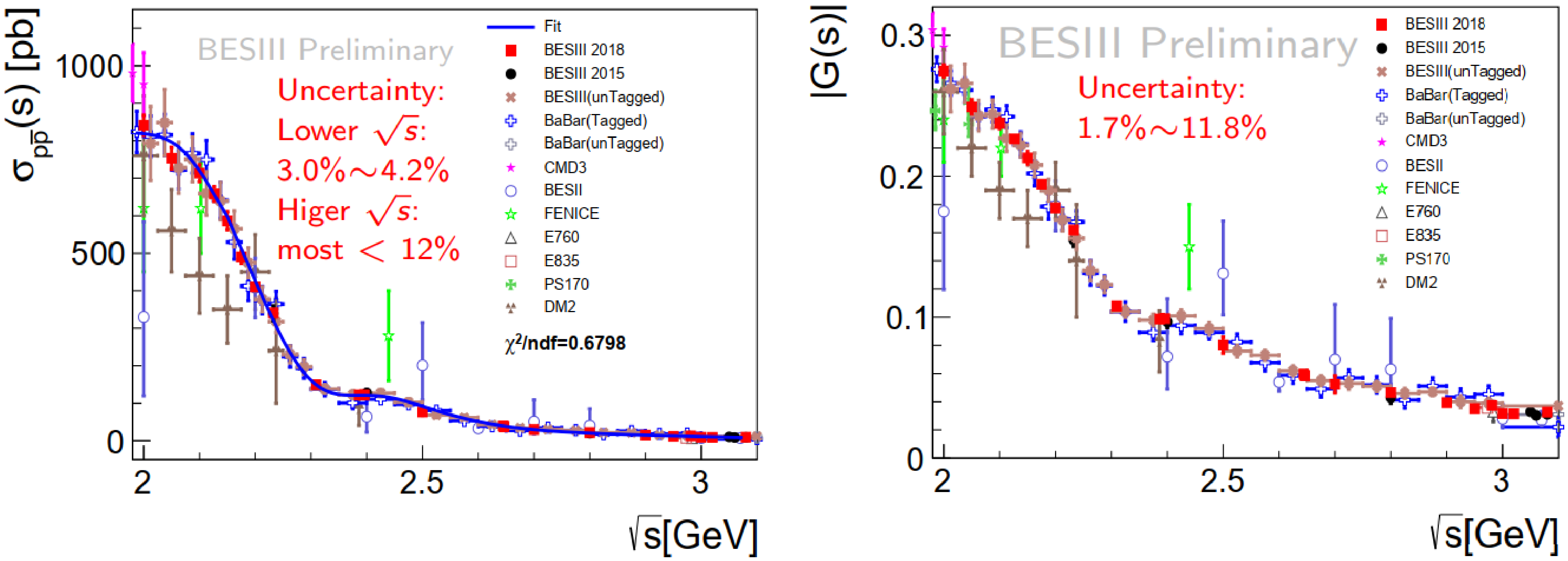

BESIII results on the cross section and effective form factor

- **Consistent with the BaBar measurement.**
- **Precision of BESIII results are significantly improved.**

- **Untagged analysis: data at [3.773-4.60] GeV, 7.4 pb-1, Phys. Rev. D 99, 092002;**
- **Tagged analysis: data at [3.773-4.60] GeV, 7.4 pb-1, under review.**

Status of proton form factors at BESIII

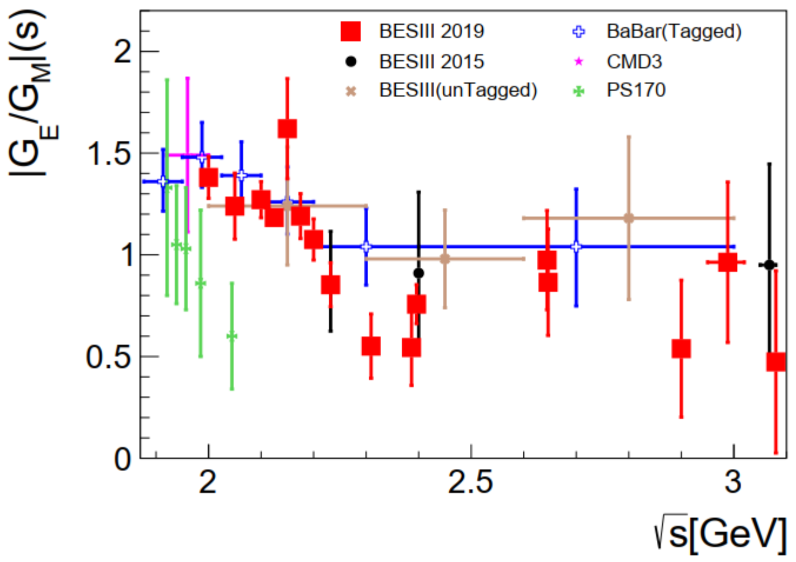

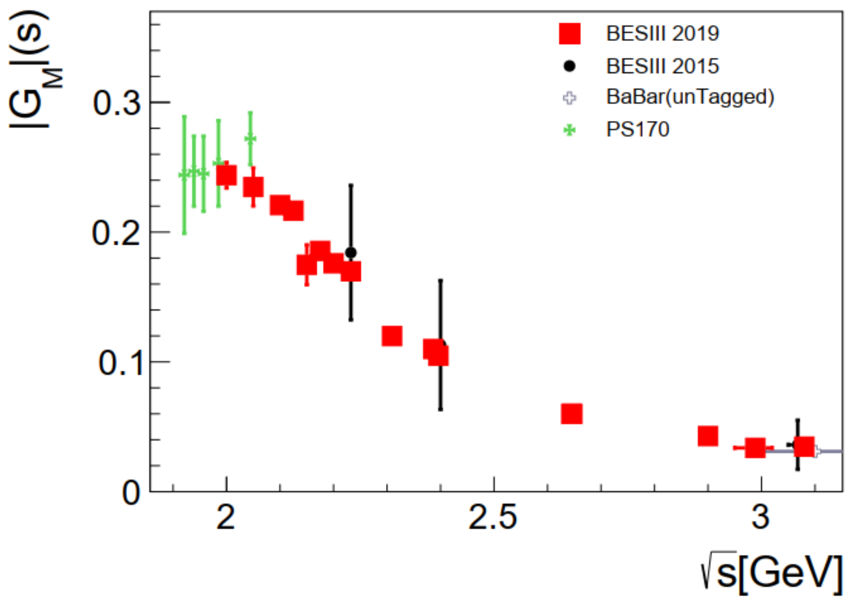

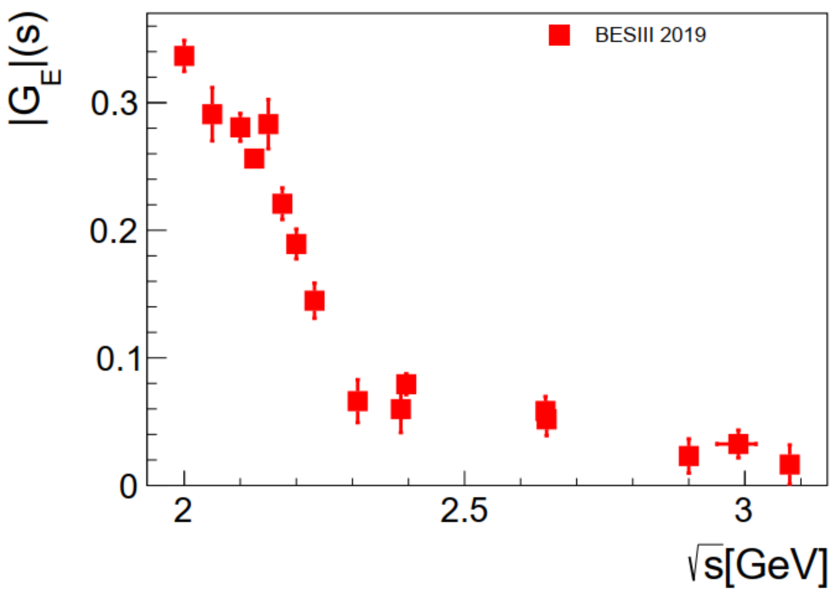

- Few results for the proton form factors exist but with big discrepancy (BaBar and PS170).
- BESIII results for the proton form factors have determined in a wide range of $\sqrt{s}$.
- BESIII results for the proton form factors ratio are consistent with BaBar results.
- **The recent results (BESIII 2019) greatly improve the precision of the proton form factors**.
  - For the first time, $|G_E|$ is measured.
  - $G_M|$ is measured with uncertainties of 1.8% to 3.6%, greatly improving the precision.
  - FF ratio $|G_E/G_M|$ is measured with total uncertainties around 10% for scan points.
  - For the first time, the accuracy of the measured FF ratio in the TL region is comparable to that of data in the SL region.

Structure in the Effective Form Factor of Proton

PRL 114, 232301 (2015) – PRC 93,035201

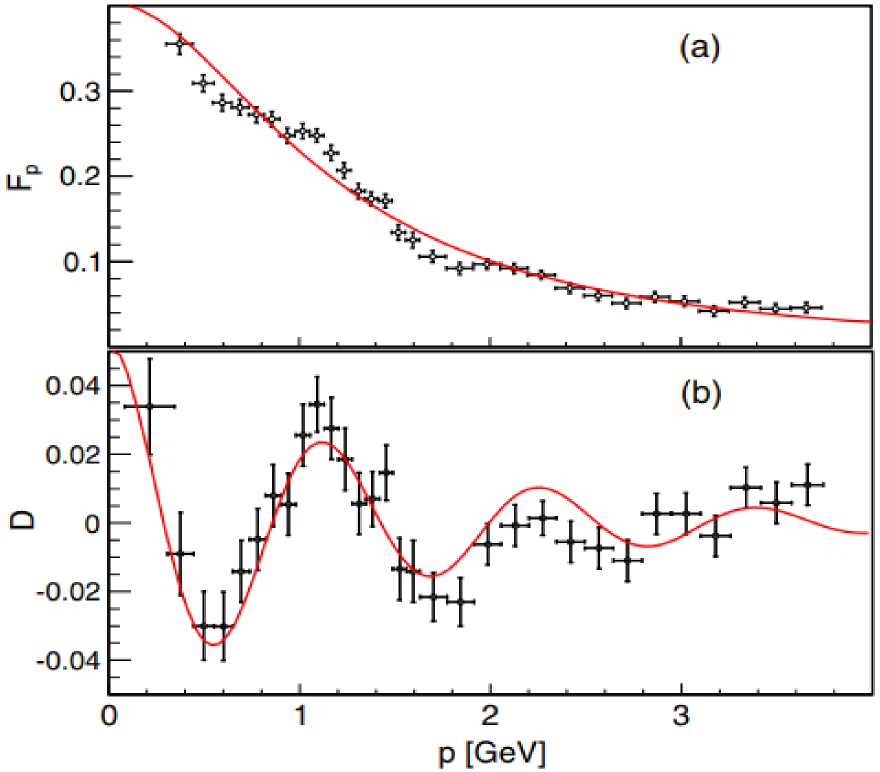

Phys. Rev. D 99, 092002

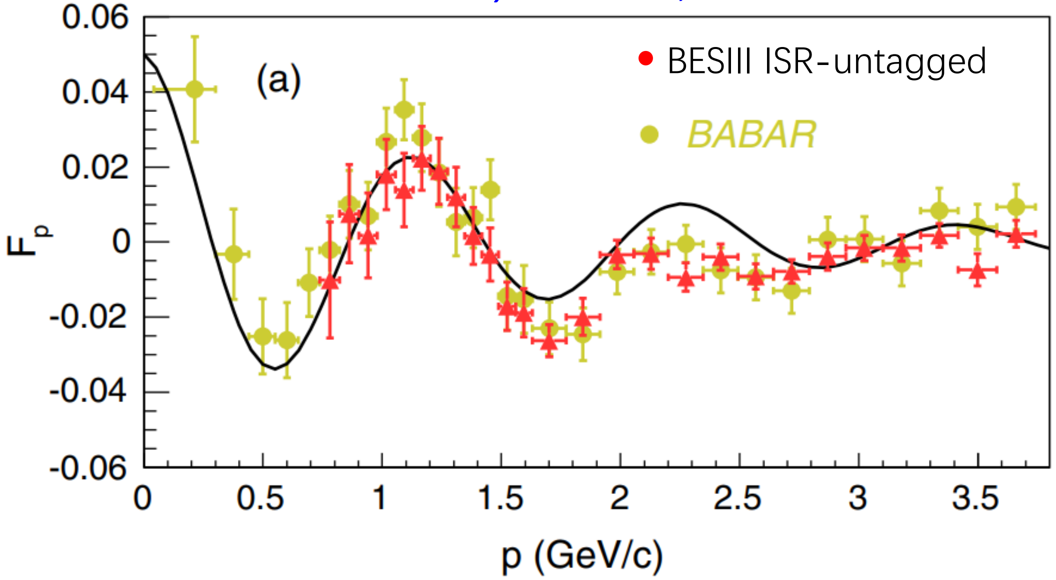

Both Babar and BESIII data are fitted with
$F_{osc}(p) = A exp(-Bp) \cos(Cp + D)$

- **First observed in Babar data, then confirmed by BESIII ISR-untagged result.**
- **A possible interference effect involving rescattering** processes at moderate kinetic energies of the outgoing hadrons (when the center-of-mass of the produced hadrons are separated by 1 fm)?
- **New structures with unknown origin,** like f(2170), or possible cusp effects by triangle graphs with virtual NΔπ, or ΔΔ threshold?

Two-Photon-Exchange

In ep scattering:

- **Rosenbluth method, which uses the analysis of angular distributions.**
- **The polarization method, which is based on the measurement of the ratio of the transverse and longitudinal polarization of the recoil proton.**
- **A possible source of the difference observed in the G_E/G_M measurements**

Phys. Rev. C 69, 022201 (2004), Phys. Rev. Lett. 88, 092301 (2002), Phys. Rev. C 71, 055202 (2005); 71,069902(E) (2005), Phys. Rev. Lett. 104, 242301 (2010)

one-photon-exchange VS two-photon-exchange

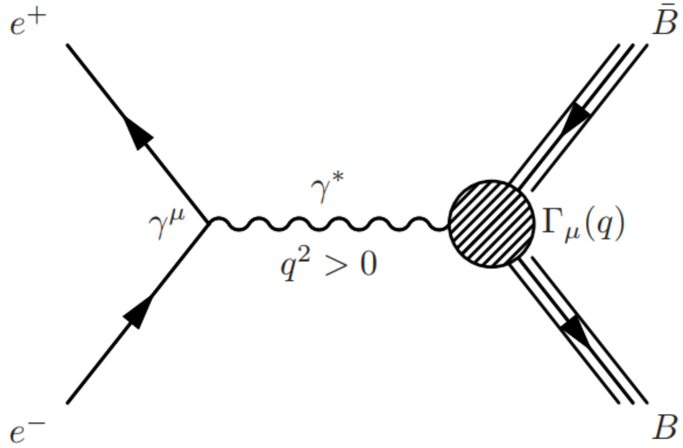

One-photon-exchange

$J^{PC}=1^{--}$

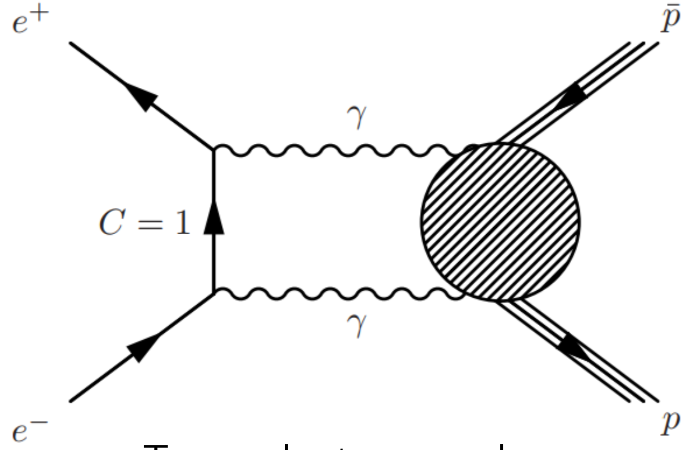

Two-photon-exchange

C=+1

- One-photon Exchange:

$$J_\mu = \frac{e^2}{q^2}\bar{u}(k_2)\gamma_\mu u(k_1)\bar{u}(p_2)[\gamma_\mu F_1(q^2) - \frac{\sigma_{\mu\nu}}{2m_p}F_2]u(p_1).$$

- Two-photon Exchange:

$$J_\mu = \frac{e^2}{q^2}\bar{u}(k_2)\gamma_\mu u(k_1)\bar{u}(p_2)[\gamma_\mu \mathcal{A}_1(s,q^2) - \frac{\sigma_{\mu\nu}}{2m_p}\mathcal{A}_2(s,q^2) + \hat{K}P_\mu \mathcal{A}_3(s,q^2)]u(p_1).$$

- Connection: 4 real amplitudes $\to$ 6 complex amplitudes.

$$\mathcal{A}_1(s,q^2) \to F_1(q^2), \mathcal{A}_2(s,q^2) \to F_2(q^2), \mathcal{A}_3(s,q^2) \to 0.$$

one-photon-exchange VS two-photon-exchange

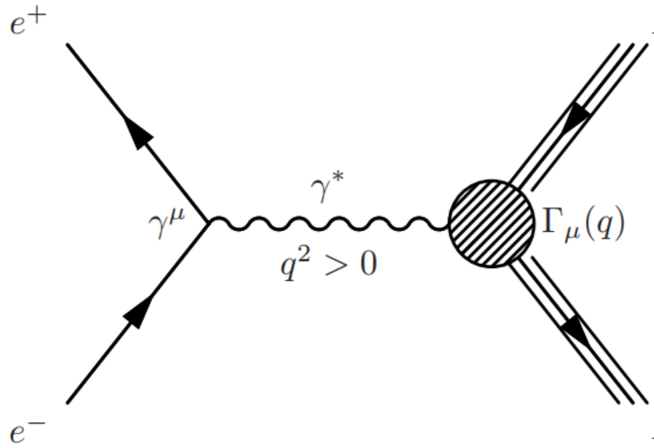

One-photon-exchange

$J^{PC}=1^{--}$

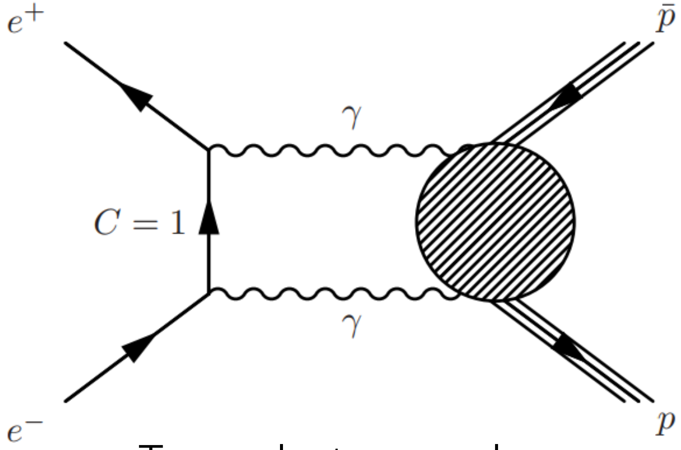

Two-photon-exchange

C=+1

- Only one-photon-exchange:

$$\frac{d\sigma}{d\Omega}(e^+ + e^- \to p + \bar{p}) \simeq a(t) + b(t)\cos^2\theta$$

- With two-photon-exchange $1\gamma \otimes 2\gamma$:

$$\frac{d\sigma^{(\mathrm{int})}}{d\Omega}(e^+ + e^- \to p + \bar{p})$$
$$= \cos\theta\left[c_0(t) + c_1(t)\cos^2\theta + c_2(t)\cos^4\theta + \cdots\right]$$

Asymmetry behavior in Babar data

PR D 87. 092005 (2013)

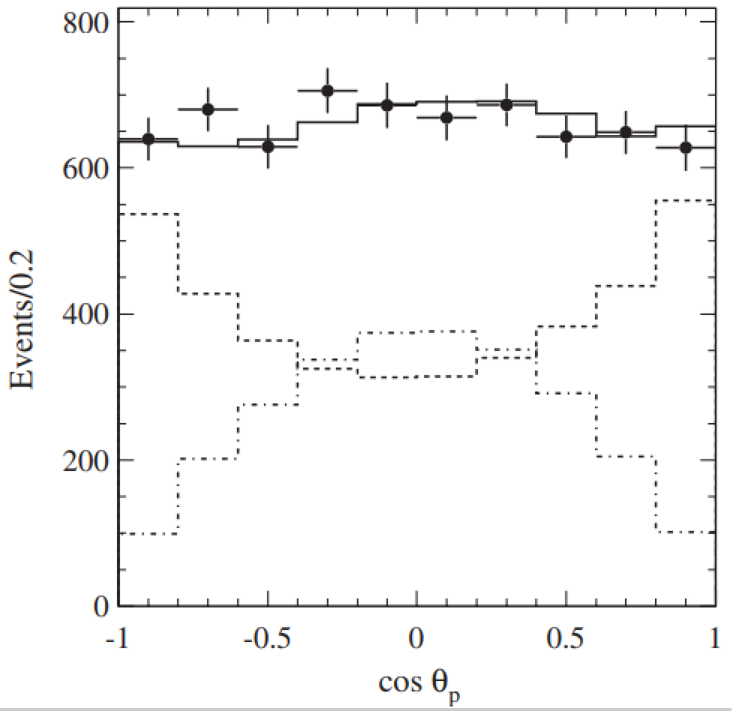

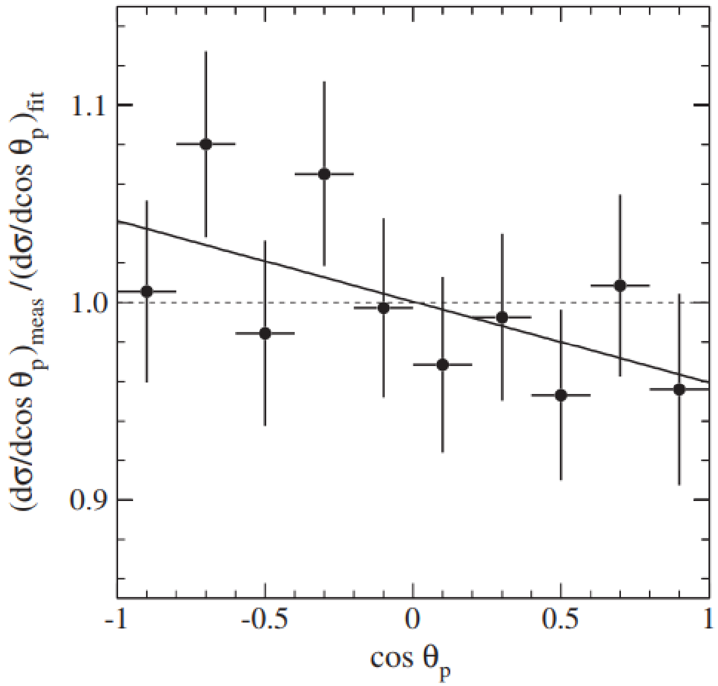

Data with M_{pp}<3.0 GeV is used, fitted with symmetry function

$$A_{\cos\theta_p} = \frac{\sigma(\cos\theta_p > 0) - \sigma(\cos\theta_p < 0)}{\sigma(\cos\theta_p > 0) + \sigma(\cos\theta_p < 0)}$$
$$= -0.025 \pm 0.014 \pm 0.003,$$

Consistent with zero within uncertainties, needs more precise measurement.

Possibility at BESIII

$\sqrt{s}$ [GeV]	Run No.	Lumi [pb^{-1}]	$\sqrt{s}$ [GeV]	Run No.	Lumi [pb^{-1}]/Events
2.0000	41729-41909	10.074	2.6444	40128-40296	34.003
2.0500	41911-41958	3.343	2.6464	40300-40435	33.722
2.1000	41588-41727	12.167	2.9000	39775-40069	105.253
2.1250	42004-43253	108.490	2.9500	39619-39650	15.9421
2.1500	41533-41570	2.841	2.9810	39651-39679	16.071
2.1750	41416-41532	10.625	3.0000	39680-39710	15.881
2.2000	40989-41121	13.699	3.0200	39711-39738	17.290
2.2324	28624-28648,	2.645	3.0800	27147-27233, 28241-28266,	31.019
	41122-41239	11.856		39355-39618	126.185
2.3094	41240-41411	21.089	J/ψ	9947-10878	225 M
2.3864	40806-40951	22.549		27255-28236,	1086 M
2.3960	40459-40769	66.869		52940-56546	4600 M

Possibility at BESIII

@2.125 GeV, $|G_E/G_M|=1.18\pm0.04\pm0.01$
(3.5% uncertainty)

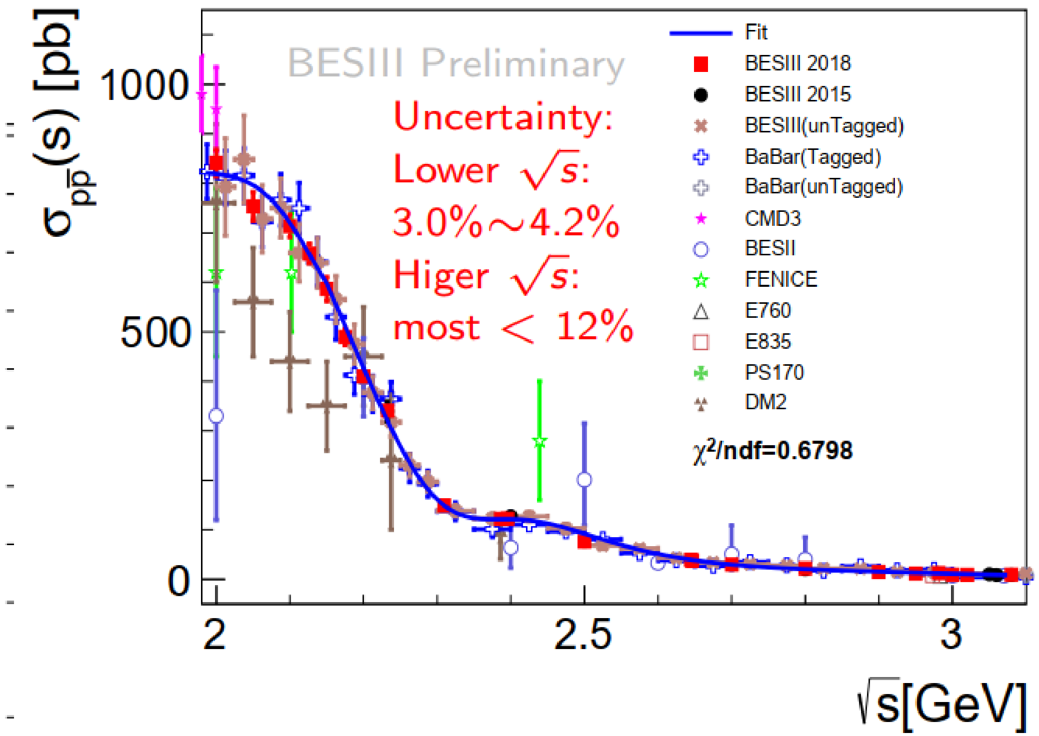

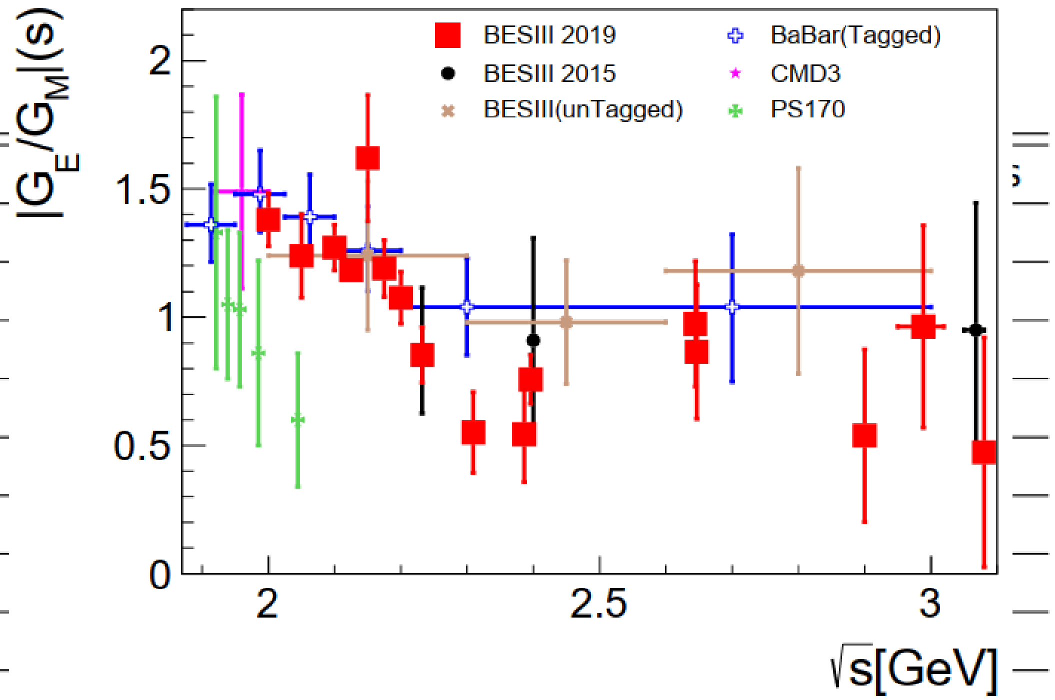

2.3864	40806-40951	22.549		9947-10878	225 M
2.3960	40459-40769	66.869	J/ψ	27255-28236,	1086 M
				52940-56546	4600 M

Provides possibility to measure the two-photon-asymmetry

MC simulation with BabayagaNLO and Phokhara for $\mu^+\mu^-$

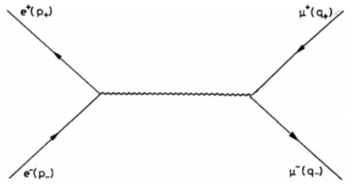

Fig. 1. Lowest order Feynman diagram for μ pair production.

+

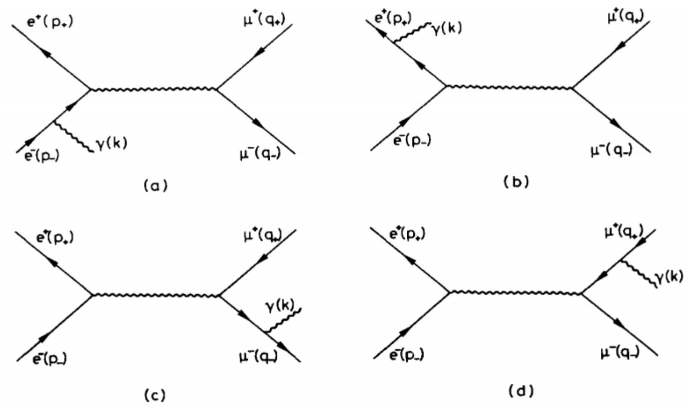

Fig. 2. Feynman diagrams for the production of a μ pair accompanied by real photon emission.

+

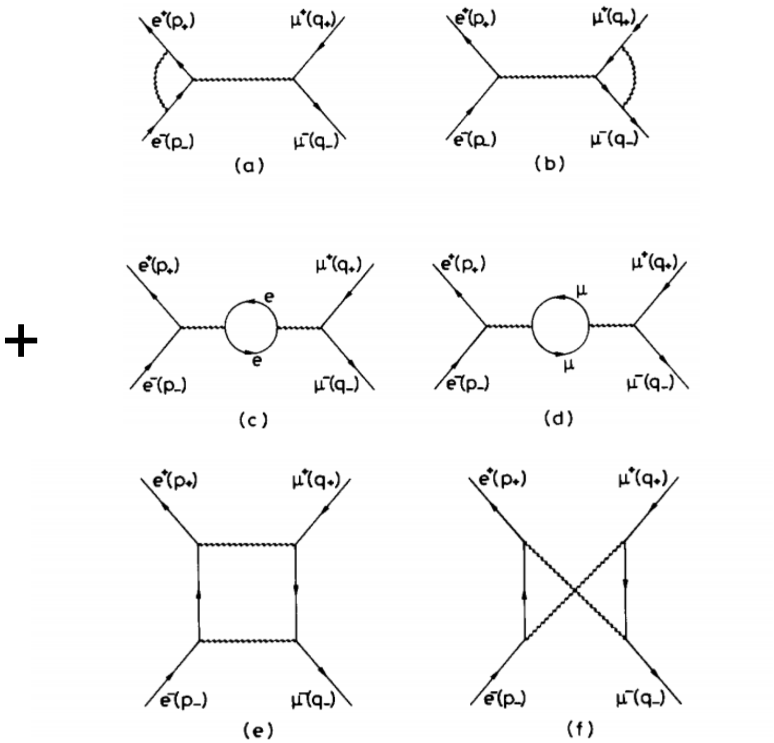

Fig. 3. Feynman diagrams for the virtual radiative corrections to μ pair production.

In Phokhra_v9, for scan mode we don't have full α^3 correction

In order to consider the α^3 correction, we sought for analytical formulas from references. However,
Reference from Berends [Nuclear Physics B63 (1973) 381-397]
and Arbuzov [Physics of Particles and Nuclei, 2011, Vol. 42, No. 1, pp.1–54] **are in disagreement**.

MC simulation with BabayagaNLO and Phokhara for $\mu^+\mu^-$

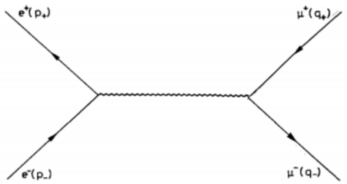

Fig. 1. Lowest order Feynman diagram for μ pair production.

+

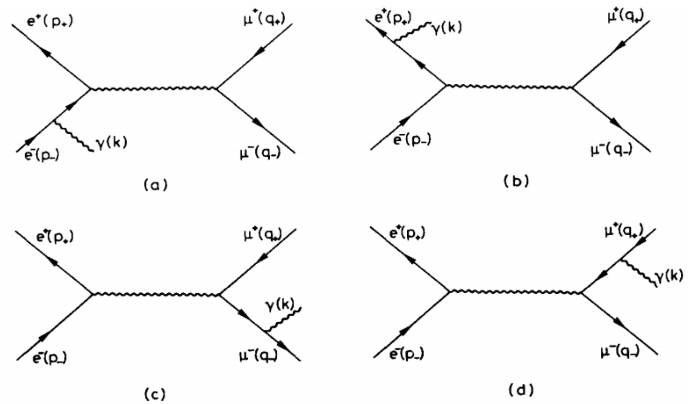

Fig. 2. Feynman diagrams for the production of a μ pair accompanied by real photon emission.

+

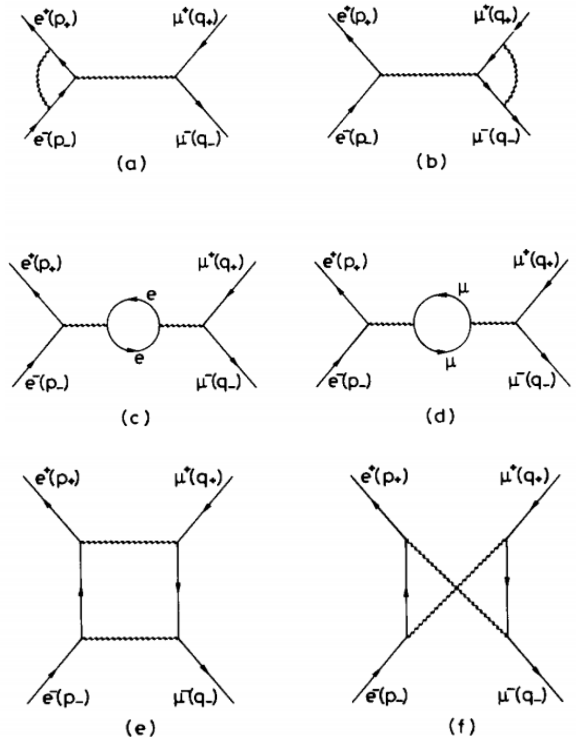

Fig. 3. Feynman diagrams for the virtual radiative corrections to μ pair production.

In Phokhra_v9, for scan mode we don't have full α^3 correction

Reference from Berends [Nuclear Physics B63 (1973) 381-397] and Hoefer [Eur. Phys. J. C 24, 51–69 (2002)] **are used for simulation**.

NOTE: 1. Provide detail checks for QED. 2. the two-photon-exchange cannot be separated from the interference between ISR and FSR due to infinity problem. So we should call "charge asymmetry" instead of single "two-photon-exchange".

MC simulation with BabayagaNLO and Phokhara for $\mu^+\mu^-$

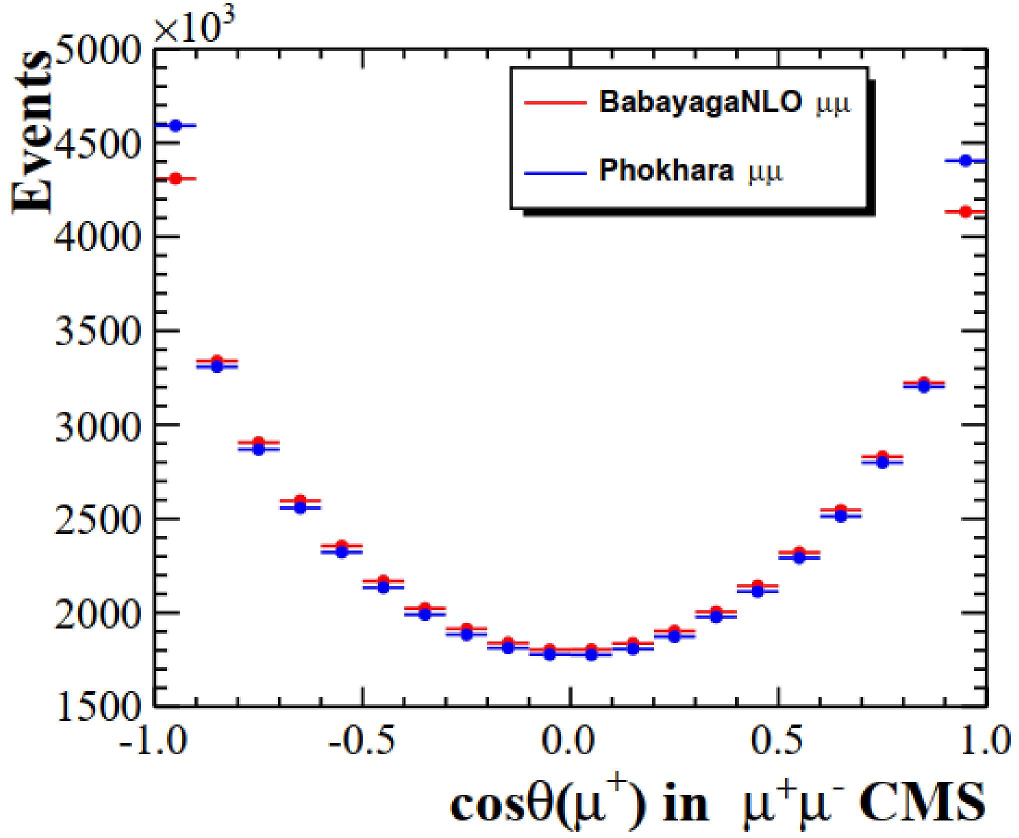

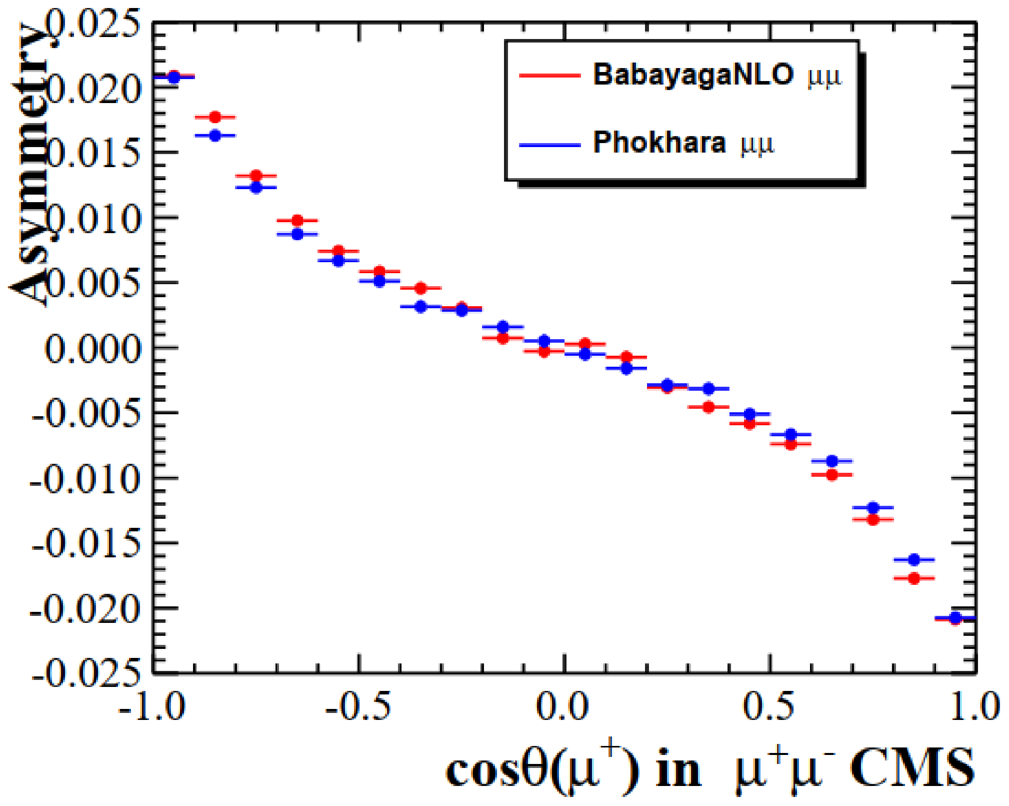

- BabayagaNLO use QED non-singlet Structure Functions method for radiation correction, more precise than Phokhara
- Phokhara (7E7 events) and BabayagaNLO (5E7 events) give consistent result,
  - BabyagaNLO: A_p =-0.0102±0.0001
  - Phokhara_10.1: A_p =-0.0098±0.0001
  - Difference within current experimental uncertainty.

MC simulation with Phokhara for $p\bar{p}$

- Assume the α^3 correction for $p\bar{p}$ is similar with $\mu^+\mu^-$. Spin ½.
- $d\sigma(2\gamma, \text{virtual})=d\sigma_{Born}(\text{Form Factors})*\delta(\text{pointlike radiative corrections})$

With BESIII form factor models.

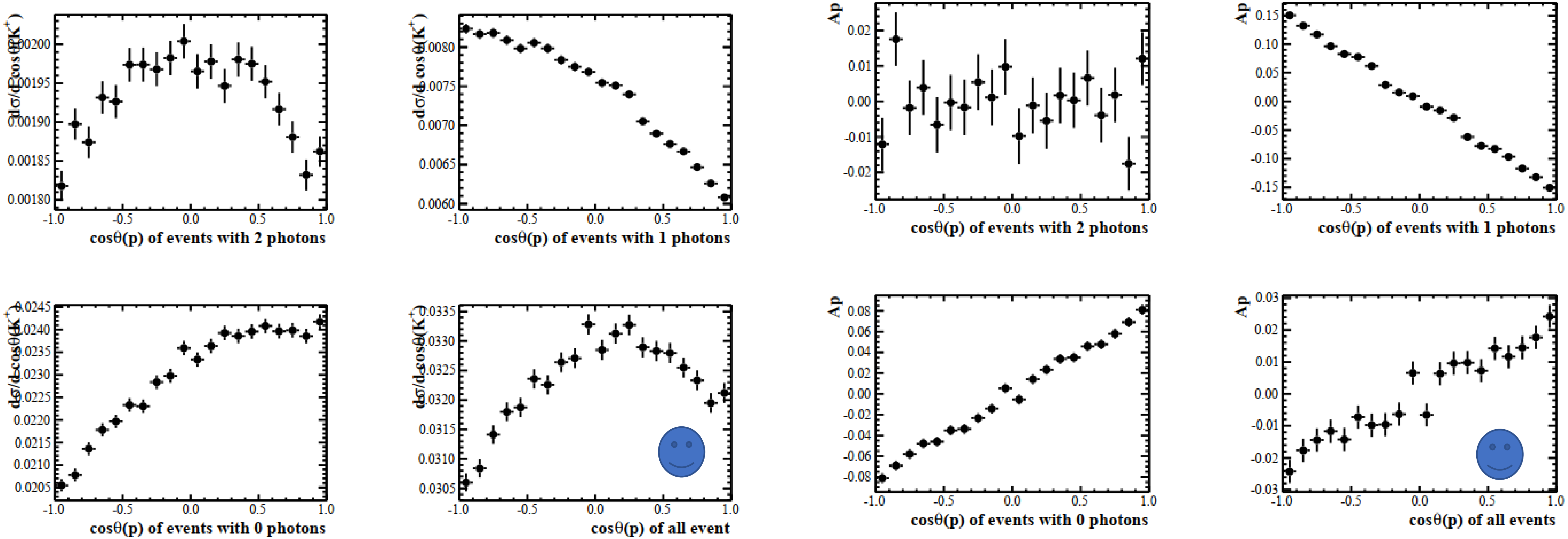

Total A_p=0.011±0.001 , same level as Babar data shows

Weighted events are used for calculation since negative weights appears

MC simulation with Phokhara for KK

- Model we use: $d\sigma(2\gamma, \text{virtual}) = d\sigma_{Born}(\text{Form Factors}) * \delta(\text{pointlike radiative corrections})$
- Reference from Jegerlehner [Eur. Phys. J. C 24, 51–69 (2002)].

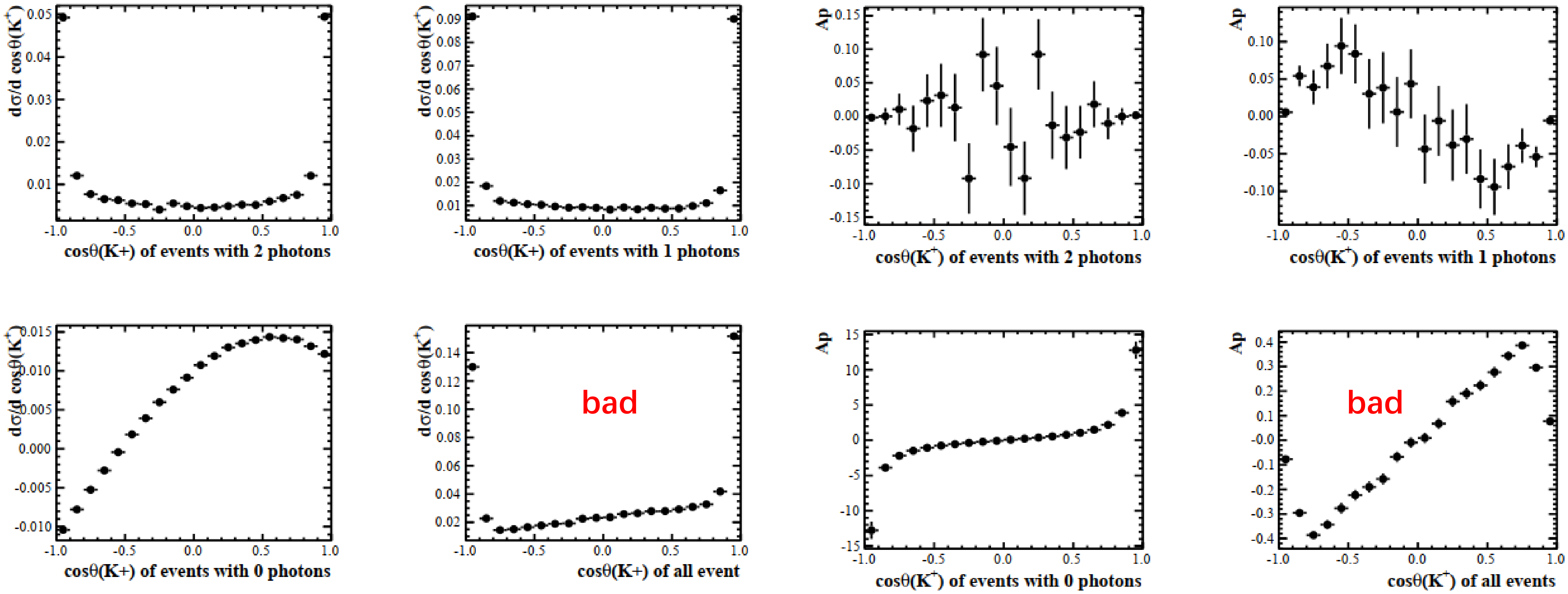

- **Meet problems, total A_p ~ 10% which is much beyond the current experimental expectation.**
- The formulas in reference papers should be revisited.

Summary

- BESIII experiment provides an excellent data for the measurement of proton form factors.
  - Two complimentary methods are used for the measurements of baryon form factors:
    - Energy scan method.
    - Initial state radiation method.
  - **The cross section has been measured in a wide range of q^2**.
  - **The form factors of proton ($|G_M|$ and $|G_E/G_M|$) are measured with unprecedented precision**.
  - **An oscillation behavior in the effective form factor of proton is obsessed**.

- Possibility measurement of charge asymmetry and MC generator are discussed.
  - Phokhara_v10 generator for $\mu^+\mu^-$ and $p\bar{p}$ are ready and hopefully to be used in the near future.
  - For $K\bar{K}$ mode, the formulas from references need to be revisited.

Thanks for your attention!


BEPC-II and BES III
Linac
Storage ring
BESIII detector
Beijing electron positron collider BEPCII
Beam energy 1.0-2.3 GeV
Energy spread: 5.16×10^{-4}
Luminosity
1×10^{33}/cm^{2}/s @ ψ(3770)
W. Gradl — New states at BES
6

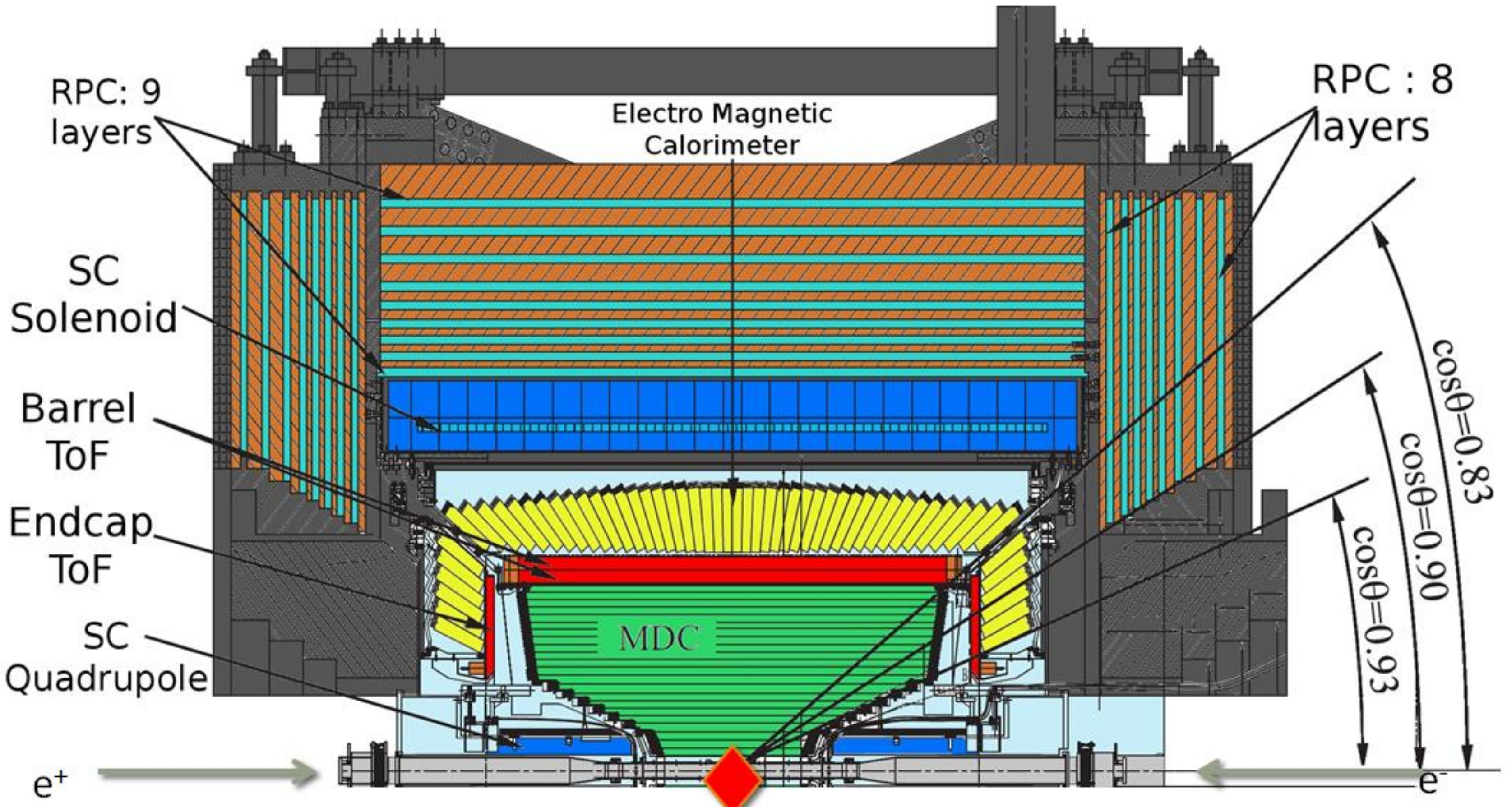
RPC: 9 layers
Electro Magnetic Calorimeter
RPC : 8 layers
SC Solenoid
Barrel ToF
Endcap ToF
SC Quadrupole
MDC
cosθ=0.83
cosθ=0.90
cosθ=0.93
e+
e-

Status of $p\bar{p}$ cross section at BESIII

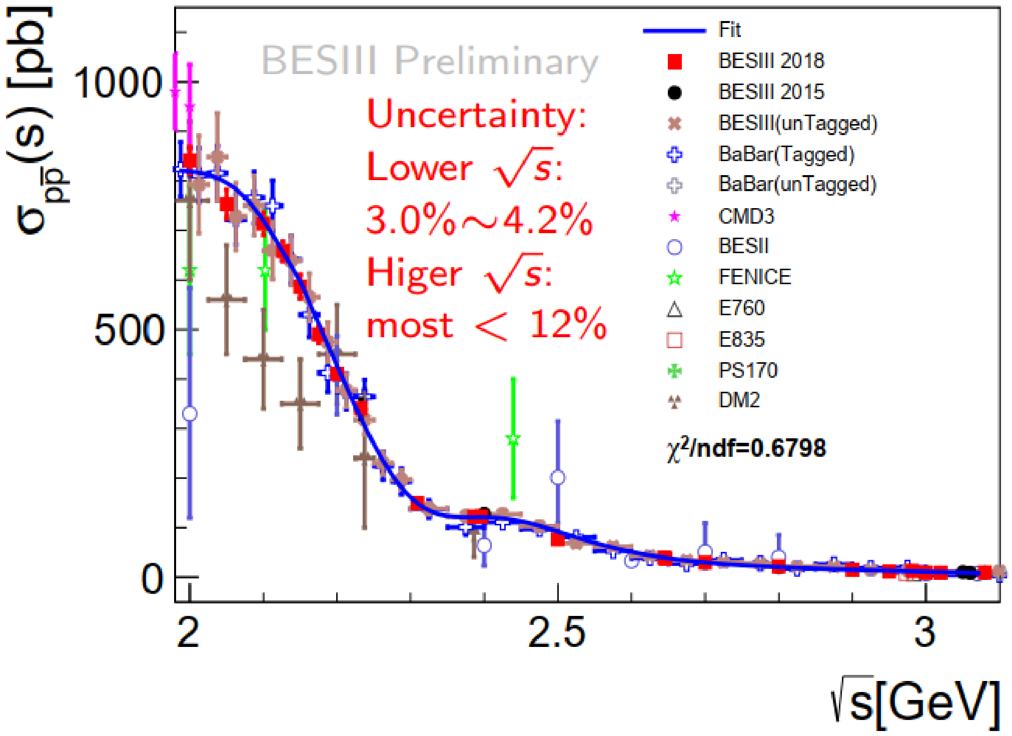

$$\sigma_{p\bar{p}}(s) = \begin{cases} \dfrac{e^{a_0}\pi^2\alpha^3}{s\left[1-e^{-\frac{\pi\alpha_s(s)}{\beta(s)}}\right]\left[1+\left(\frac{\sqrt{s}-2m_p}{a_1}\right)^{a_2}\right]}, \\ \qquad \sqrt{s} \leq 2.3094\ \mathrm{GeV}, \\ \dfrac{2\pi\alpha^2\beta(s)C\left[2+\left(\frac{2m_p}{\sqrt{s}}\right)^2\right]e^{2a_3}}{3s^5\left[4\ln^2\left(\frac{\sqrt{s}}{a_4}\right)+\pi^2\right]^2}, \\ \qquad \sqrt{s} > 2.3094\ \mathrm{GeV}, \end{cases}$$

BESIII results on the cross section and effective form factor

- **Direct scan method:**
  - **2012 data, 156.7 pb-1, PRD 91,112004 (2015);**
  - **2015 data, 668.5 pb-1, arXiv:1905.09001 (most recent and precise results.)**
- **Initial state radiation method:**
  - **Untagged analysis: data at [3.773-4.60] GeV, 7.4 pb-1, Phys. Rev. D 99, 092002;**
  - **Tagged analysis: data at [3.773-4.60] GeV, 7.4 pb-1, under review.**